Fluorescent probe: complexation of Fe^{3+} with the *myo*-inositol 1,2,3-trisphosphate motif†

David Mansell,[a] Nicholas Rattray,[a] Laura L. Etchells,[a] Carl H. Schwalbe,[b] Alexander J. Blake,[c] Elena V. Bichenkova,[a] Richard A. Bryce,[a] Christopher J. Barker,[d] Alvaro Díaz,[e] Carlos Kremer[f] and Sally Freeman*[a]

Received (in Cambridge, UK) 30th May 2008, Accepted 3rd September 2008
First published as an Advance Article on the web 29th September 2008
DOI: 10.1039/b809238a

Natural *myo*-inositol phosphate antioxidants containing the 1,2,3-trisphosphate motif bind Fe^{3+} in the unstable penta-axial conformation.

The natural product *myo*-inositol 1,2,3-trisphosphate (**1**)[1] (Ins(1,2,3)P_3, cellular concentration $\leq$ 10 μM[1]) is a potent iron-chelator (apparent K_i = 9.0 × 10^{-19} M) and antioxidant, completely inhibiting iron-catalysed hydroxyl radical ($HO^{\bullet}$) formation.[2,3] Our recent potentiometric studies demonstrate that, unlike the more abundant *myo*-inositol hexakisphosphate (InsP_6 ≈ 20 μM[4]), Ins(1,2,3)P_3 fulfils the requirements of a safe, low molecular weight biological Fe^{3+} shuttle.[5,6] Under conditions of excess Mg^{2+} (*e.g.* cytosolic and nuclear regions of mammalian cells), a negligible proportion of InsP_6 is bound to Fe^{3+}.[7] In contrast, Fe^{3+} remains fully complexed with Ins(1,2,3)P_3, both under Mg^{2+}-rich conditions and in acidic, Ca^{2+}-rich media such as in lysosomes.[5] It was also predicted that iron bound to Ins(1,2,3)P_3 must be Fe^{3+}, since its affinity for Fe^{2+} is not high enough to allow interaction in the presence of excess cellular Mg^{2+}. Although the biological relevance of Ins(1,2,3)P_3 binding to iron is clear, the structure of its complex is uncertain and forms the subject of this paper. We have previously shown that the crystal structure of cyclohexylammonium Ins(1,2,3)P_3 adopted the expected stable penta-equatorial chair conformation (**1A**).[8] Here using density functional calculations at the UB3LYP/6-31+G* level,[9] we have modelled **1** as the hexamethyl phosphoester, to represent protonation and counterion/solvent screening effects. From the optimal geometries, we have estimated that **1A** is 8 kcal mol^{-1} more favourable in energy than the penta-axial conformation **1B** (Scheme 1). This energetic preference increases to 30 kcal mol^{-1} for the hexaanionic forms of **1A** and **1B**.

It has been proposed by Phillippy and Graf that the complex of Fe^{3+} with Ins(1,2,3)P_3 adopts the penta-axial conformation (**1B**):[10] the phosphate groups are orientated closer together, allowing Ins(1,2,3)P_3 to complex to Fe^{3+} with hexa-coordination using two terminal oxygens from each phosphate. This structure was based on the observation that azide has no effect on the visible absorption spectrum of Ins(1,2,3)P_3–Fe^{3+}, in contrast to the marked shift observed for Ins(1,2,6)P_3–Fe^{3+} due to water displacement.[10] To explore this further, we employed ^{1}H NMR studies to confirm the penta-equatorial conformation of Ins(1,2,3)P_3 in the absence of Fe^{3+}. However, no structural information on its Fe^{3+} complex could be obtained due to peak broadening. An alternative experimental approach to conformational studies of **1** was therefore required.

We have recently developed a fluorescent probe based on the acid-triggered conformational flip of an orthoformate constrained *myo*-inositol ring using pyrene excimer fluorescence.[11,12] This methodology inspired the design of a fluorescent probe to study the Ins(1,2,3)P_3 motif, using Fe^{3+} complexation as the potential trigger for conformational change. 4,6-Bis-*O*-pyrenoyl-*myo*-inositol 1,2,3,5-tetrakisphosphate (**2**) has been synthesised as a fluorescent probe to monitor whether the ring flip of *myo*-inositol occurs upon association with Fe^{3+} (Scheme 2). If Fe^{3+} binds to the more stable penta-equatorial chair conformation (**2A**), a monomer emission signal of the pyrene groups would be expected. If Fe^{3+} binds to the less stable penta-axial conformation (**2B**) this will favour π–π stacking of the pyrene groups promoting excimer fluorescence (Scheme 2).

The 1,2,3,5-tetrakisphosphate *myo*-inositol derivative was chosen over the Ins(1,2,3)P_3 derivative due to the significantly shorter synthesis of the fluorescent probe. We are confident that *myo*-inositol 1,2,3,5-tetrakisphosphate is a good model of the 1,2,3-trisphosphate motif as it possesses similar anti-oxidant properties and Fe^{3+} affinity to Ins(1,2,3)P_3.[2] The synthesis of

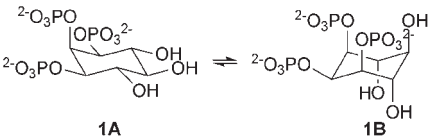

Scheme 1 Penta-equatorial (**1A**) and penta-axial (**1B**) conformations of Ins(1,2,3,)P_3.

[a] *School of Pharmacy & Pharmaceutical Sciences, University of Manchester, Oxford Road, Manchester, UK M13 9PT. E-mail: sally.freeman@manchester.ac.uk; Fax: 44 161 275 2396; Tel: 44 161 275 2366*
[b] *School of Life and Health Sciences, Aston University, Birmingham, UK B4 7ET*
[c] *School of Chemistry, The University of Nottingham, University Park, Nottingham, UK NG7 2RD*
[d] *Rolf Luft Research Center for Diabetes and Endocrinology, Karolinska Institutet, SE-171 76 Stockholm, Sweden*
[e] *Cátedra de Inmunología, Facultad de Química/Ciencias, Universidad de la República, Avenida Alfredo Navarro 3051, CP 11600 Montevideo, Uruguay*
[f] *Cátedra de Química Inorgánica, Departamento Estrella Campos, Facultad de Química, Universidad de la República, CC 1157 Montevideo, Uruguay*

† Electronic supplementary information (ESI) available: Coordinates and absolute energies for **7A** and **7B**. Crystal data for **3·CDCl$_3$**. CCDC 690016. For ESI and crystallographic data in CIF or other electronic format, see DOI: 10.1039/b809238a

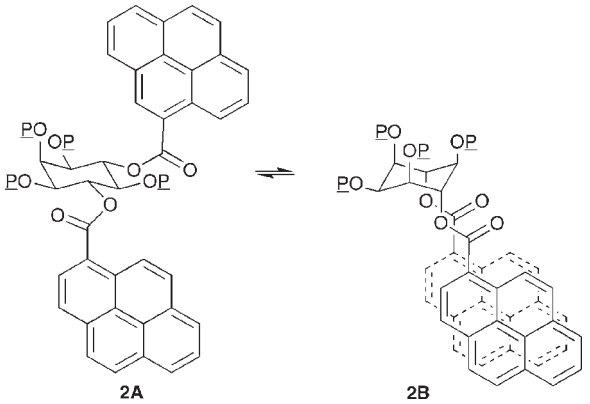

Scheme 2 Penta-equatorial (**2A**) and penta-axial (**2B**) conformations of 4,6-bispyrenoyl Ins(1,2,3,5)P_4. P = PO_3^{2-}.

(**2**) (Scheme 3) commences with 4,6-bispyrenoyl-*myo*-inositol 1,3,5-orthoformate (**3**), the excimer fluorescent properties of which have been reported by our group.[11,12]

Fortuitously, crystals of (**3·CDCl$_3$**) were obtained and its X-ray structure is described (Fig. 1).‡ The crystal structure elegantly demonstrates the π–π stacking of the pyrene rings, and hence rationalises its fluorescent properties. Bond angles at orthoformate oxygen atoms O1, O3 and O5 are approximately tetrahedral in **3**, but the angle at O2, which bears the bulky silyl group, is opened to 122.35(10)°, even wider than the value of 121.01(2)° for the corresponding angle in the related feruloyl derivative.[13] In contrast to the feruloyl derivative, the two large pyrene rings of **3** are efficiently stacked (Fig. 1A), the dihedral angle between ring planes being only 3.29(3)°. The pyrene rings of **3** resemble a clamshell hinged along the C18···C20 and C35···C37 side (Fig. 1B). C18 and C20 are only 3.307(2) and 3.276(2) Å out of the least-squares plane through all ring carbon atoms from C32 to C47, but on the far side the distance from this plane increases to 3.578(2) and 3.592(2) Å for C25 and C27. Since the stacking separation exceeds the theoretical 2.52 Å between adjacent identical axial substituents on an undistorted cyclohexane ring, and the average 2.54 Å distance between axial H atoms observed

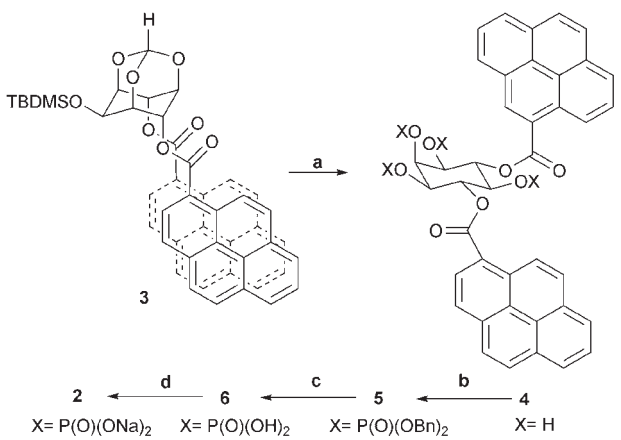

Scheme 3 Synthesis of the fluorescent probe 4,6-bis-pyrenoyl-*myo*-inositol 1,2,3,5-tetrakisphosphate (**2**): (a) *p*-toluenesulfonic acid, THF : MeOH (2 : 1); (b) i, dibenzyl *N*,*N*-diisopropylphosphoramidite, 0.45 M 1*H*-tetrazole, MeCN; ii, *m*-CPBA, DCM; (c) H_2/Pd-C, ethanol; (d) Dowex 50-X8 resin, mesh 20–50, Na^+ form, elution with water.

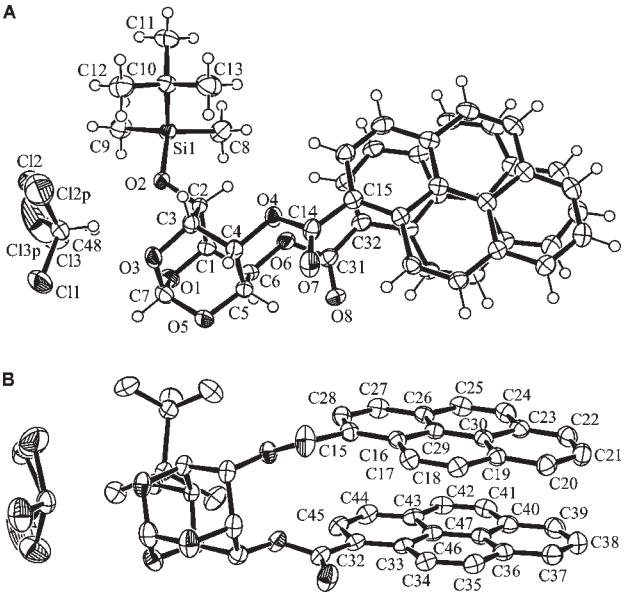

Fig. 1 Complementary ORTEP[16] diagrams of (**3·CDCl$_3$**) showing the atom numbering scheme. Ellipsoids are drawn at the 50% probability level. In **B** the H atoms and selected atom labels are omitted for clarity.

in cyclohexane,[14] adjustments are required. These start with the splaying effect of expansion above the tetrahedral angle in C4–C5–C6 to 113.75(13)°, C5–C4–O4 to 110.65(12)° and C5–C6–O6 to 114.51(14)°. Twisting about the three rotatable bonds between C4 and C15 and those between C6 and C32 results is a steady increase in separation distance from 2.565(2) Å for C4···C6 to 2.804(2) Å for O4···O6 and 3.616(2) Å for C14 and C31 that still allows the pyrene rings to be nearly parallel.

The orthoformate and *tert*-butyldimethylsilyl protecting groups in **3** were removed simultaneously in the presence of *p*-toluenesulfonic acid[15] to give tetrol **4**, which was treated with dibenzyl *N*,*N*-diisopropylphosphoramidite, followed by oxidation with *m*-chloroperoxybenzoic acid to give **5**. Benzyl deprotection of **5** was achieved by catalytic hydrogenation to generate the free acid **6**, which was converted to the sodium salt (**2**) (Scheme 3).§

The fluorescence emission spectra of **2** were recorded in the absence and presence of Fe^{3+} (Fig. 2). The emission spectrum of **2** alone gave rise to blue fluorescence observed at 386 nm and attributed to the locally excited state of the pyrene monomer. The presence of Fe^{3+} caused a marked change in fluorescence, with the observation of substantial quenching of the fluorescence of the locally excited state at 386 nm accompanied by the appearance of a new broad emission band at 510 nm (green fluorescence). This was attributed to the excimer emission of the two closely located pyrene groups achieved in the penta-axial conformation (**2B**).

Due to the quenching properties of Fe^{3+}, the fluorescence emission spectrum of **2** was also recorded in the presence of Ga^{3+} (d^{10}), a non-quenching analogue of Fe^{3+} (high-spin d^5).[17–19] Both cations have the same charge, similar ionic radii and are known to form isomorphous hexa-coordinate complexes.[20] Based on this, Ga^{3+} was predicted to behave similarly to Fe^{3+} with respect to its binding to the fluorescent probe. This was indeed the case and a similar emission spectrum was recorded in the presence of Ga^{3+}

 This journal is © The Royal Society of Chemistry 2008

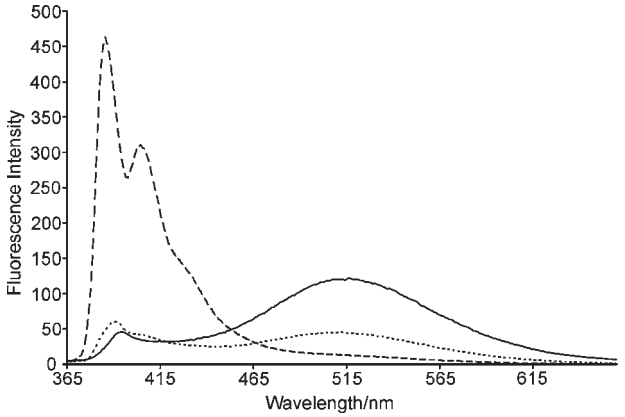

Fig. 2 Emission spectra of 4,6-bispyrenoyl Ins(1,2,3,5)P_4 (**2**) in the absence (- - -) and presence (···) of Fe^{3+} (1 equiv.) and the presence (—) of Ga^{3+} (1 equiv.). Spectra were recorded at a concentration of 1 mM in methanol at 20 °C. Excitation and emission slit widths were 3 nm (absence of metal) and 5 nm (presence of metal).

(Fig. 2). The excimer peak was observed at 515 nm with an intensity more than double that observed with Fe^{3+}. This evidence supports the general principle that Fe^{3+} binds to the penta-axial conformation.[10]

To obtain detailed structural information, calculations on high-spin Fe^{3+} complexes of penta-axial hexamethyl phosphoester at the UB3LYP/6-31+G* level were performed. Conforming to the 1 : 1 Ins(1,2,3)P_3–Fe^{3+} stoichiometry suggested by potentiometric titrations[5] and the absence of water within the coordination sphere implied by azide competition experiments,[10] we obtained after conformational searching two essentially isoenergetic Fe^{3+}-coordinating penta-axial geometries, **7A** and **7B** (Fig. 3). Distinct from the structure suggested by Phillippy and Graf,[10] for which we were unable to detect a stable minimum, both **7A** and **7B** involve inositol *phosphoester* oxygens as well as terminal oxygens in the coordination of Fe^{3+}. Similar Fe^{3+}-coordination is predicted for hexa-anionic Ins(1,2,3)P_3. Structure **7A** adopts a distorted tetrahedral coordination involving one phosphoester and three terminal oxygens in the coordination of Fe^{3+}. Structure **7B**, which is 0.1 kcal mol^{-1} higher in energy than **7A**, adopts a distorted trigonal bipyramidal coordination around Fe^{3+} involving participation of two phosphoester and three terminal oxygens. Further experimental studies are required to unambiguously establish the structure of the Ins(1,2,3)P_3–Fe^{3+} complex.

This study provides evidence that Fe^{3+} binding to *myo*-inositol phosphates possessing the 1,2,3-trisphosphate motif is achieved by adopting the penta-axial conformation. Interest surrounds the precise biological function of Ins(1,2,3)P_3 (**1**), and in future research the fluorescent probe may be of use to study the behaviour of **1** in cells.

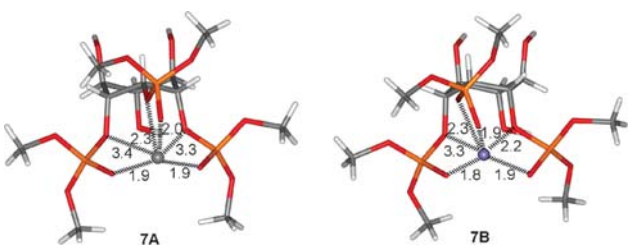

Fig. 3 Optimal UB3LYP/6-31+G* geometries (Å) of the hexamethyl phosphoester of Ins(1,2,3)P_3–Fe^{3+} (**1**) in the high-spin state.

N.R. thanks Morvus Technologies for a CASE studentship. We thank ESPRC for award of a diffractometer.

Notes and references

‡ Crystal data for **3·CDCl$_3$**: $C_{47}H_{38}O_8Si{\cdot}CDCl_3$, M = 880.25, triclinic, space group $P\bar{1}$, a = 11.1679(9), b = 11.6838(9), c = 16.9249(13) Å, α = 72.420(2), β = 81.387(2), γ = 87.634(2)°, V = 2081.5(3) Å^3, Z = 2, T = 150 K, Z = 2, D = 1.404 (calc.), μ = 0.306 mm^{-1}. 18 993 reflections measured, 9307 unique (R_{int} = 0.0075); after final refinement R = 0.041 for 6716 reflections with $F_o > 4\sigma(F_o)$, w$R(F^2)$ = 0.114 for all 9307 reflections.

§ For **2**, δ_H (500 MHz, D_2O, water supp.): 9.12 (2H, d, J 9.4 Hz, Pyr), 8.90 (2H, d, J 7.6 Hz, Pyr), 8.76–8.25 (14H, m, Pyr), 6.04 (2H, t, J_{AA} 9.9 Hz, H-4/6), 5.34 (1H, br d, J_{PH} 10.1 Hz, H-2), 4.91 (1H, dt ≈ br q, $J_{AA} \approx J_{PH}$ 8.7 Hz, H-5), 4.79–4.68 (2H, br t, $J_{AA} \approx J_{PH}$ 7.2 Hz, H-1/3). δ_P (121 MHz, D_2O): 1.79 (1P), −0.09 (2P), −1.08 (1P). IR data: ν_{max}/cm^{-1} 1703 (C═O); 1257 (m), 1226 (m), 1195 (m), (P═O); 1082 (s), 1048 (s), 1018 (s) (P–O–Bn).

1 (*a*) C. J. Barker, P. J. French, A. J. Moore, T. Nilsson, P. O. Berggren, C. M. Bunce, C. J. Kirk and R. H. Michell, *Biochem. J.*, 1995, **306**, 557–564; (*b*) F. M. McConnell, S. B. Shears, P. J. L. Lane and M. S. Scheibel, *Biochem. J.*, 1992, **284**, 447–455.
2 I. D. Spiers, C. J. Barker, S.-K. Chung, Y.-T. Chang, S. Freeman, J. M. Gardiner, P. H. Hirst, P. A. Lambert, R. H. Michell and D. R. Poyner, *Carbohydr. Res.*, 1996, **282**, 81–99.
3 I. D. Spiers, S. Freeman, D. R. Poyner and C. H. Schwalbe, *Tetrahedron Lett.*, 1995, **36**, 2125–2128.
4 A. J. Letcher, M. J. Schell and R. F. Irvine, *Biochem. J.*, 2008, DOI: 10.1042/BJ20081417.
5 N. Veiga, J. Torres, D. Mansell, S. Freeman, S. Domínguez, C. J. Barker, A. Díaz and C. Kremer, *J. Biol. Inorg. Chem.*, DOI: 10.1007/s00775-008-0423-2.
6 C. J. Barker, J. Wright, P. J. Hughes, C. J. Kirk and R. H. Michell, *Biochem. J.*, 2004, **380**, 465–473.
7 J. Torres, S. Domínguez, M. F. Cerdá, G. Obal, A. Mederos, R. F. Irvine, A. Díaz and C. Kremer, *J. Inorg. Biochem.*, 2005, **99**, 828–840.
8 I. D. Spiers, S. Freeman and C. H. Schwalbe, *J. Chem. Soc., Chem. Commun.*, 1995, 2219–2220.
9 M. J. Frisch and co-workers, *Gaussian 03*, 2004. See ESI for full citation†.
10 B. Q. Phillippy and E. Graf, *Free Radical Biol. Med.*, 1997, **22**, 939–946.
11 M. Kadirvel, E. V. Bichenkova, A. D'Emanuele and S. Freeman, *Chem. Lett.*, 2006, **35**, 868–869.
12 M. Kadirvel, B. Arsic, S. Freeman and E. V. Bichenkova, *Org. Biomol. Chem.*, 2008, **6**, 1966–1972.
13 A. Hosoda, Y. Ozaki, A. Kashiwada, M. Mutoh, K. Wakabayashi, K. Mizuno, E. Nomura and H. Taniguchi, *Bioorg. Med. Chem.*, 2002, **10**, 1189–1196.
14 R. Kahn, R. Fourme, D. Andre and M. Renaud, *Acta Crystallogr., Sect. B: Struct. Crystallogr. Cryst. Chem.*, 1973, **29**, 131–138.
15 T.-H. Kim and A. B. Holmes, *J. Korean Chem. Soc.*, 2006, **50**, 129–136.
16 C. K. Johnson, *ORTEP-II*, Report ORNL-5138, Oak Ridge National Laboratory, Oak Ridge, TN, USA, 1976.
17 B. Bodenant, F. Fages and M. H. Delville, *J. Am. Chem. Soc.*, 1998, **120**, 7511–7519.
18 F. Fages, B. Bodenant and T. Weil, *J. Org. Chem.*, 1996, **61**, 3956–3961.
19 F. Fages, S. Leroy, T. Soujanya and J.-E. Sohna Sohna, *Pure Appl. Chem.*, 2001, **73**, 411–414.
20 B. A. Borgias, S. J. Barclay and K. N. Raymond, *J. Coord. Chem.*, 1986, **15**, 109–123.